Design of Efficient Partitioned Procedures for the Transient Solution of Aeroelastic Problems

Serge Piperno* — **Charbel Farhat****

* *CERMICS – INRIA (project Caiman)*
2004, route des Lucioles, B.P. 93
F-06902 Sophia Antipolis Cedex
Serge.Piperno@sophia.inria.fr

** *Department of Aerospace Engineering Sciences*
and Center for Aerospace Structures
University of Colorado at Boulder
Boulder, CO 80309-0429, U.S.A.

ABSTRACT. *We consider the problem of solving large-scale non-linear dynamic aeroelasticity problems in the time-domain using a fluid-structure partitioned procedure. We present a mathematical framework for assessing some important numerical properties of the chosen partitioned procedure, and predicting its performance for realistic applications. Our analysis framework is based on the estimation of the energy that is artificially introduced at the fluid-structure interface by the staggering process that is inherent to most partitioned solution methods. This framework provides a powerful means for the construction of more accurate and stable partitioned methods. Using two- and three-dimensional, transonic and supersonic, wing and panel aeroelastic applications, we validate this framework and highlight its impact on the design and selection of a staggering algorithm for the solution of coupled fluid-structure equations.*

RÉSUMÉ. *Nous présentons une méthode qualitative d'évaluation d'algorithmes de couplage pour la simulation numérique de systèmes aéroélastiques non linéaires. Cette évaluation, fondée sur la mesure de l'énergie artificiellement produite à l'interface fluide-structure, est un outil puissant pour la construction de nouvelles méthodes plus efficaces. Nous en validons les résultats et démontrons les possibilités sur des écoulements autour de structures déformables.*

KEY WORDS : *Fluid-structure interactions, coupling algorithm, staggered partitioned procedure, energy conservation, evaluation and design criterion.*

MOTS-CLÉS : *Interactions fluide-structure, algorithme de couplage, méthode décalée, conservation de l'énergie, critère d'évaluation et de construction.*

1. Introduction

Wing flutter, fighter tail buffeting and flow induced pipe vibrations are examples of fluid-structure interaction phenomena that are of great concern to aerospace, mechanical, and civil engineering. Since the underlying fluid system is represented by a non-linear model (i.e. the Euler or Navier-Stokes equations), these problems are referred to as *non-linear transient* aeroelastic problems.

A non-linear transient aeroelastic problem where the fluid domain boundaries undergo a motion with a large amplitude can be formulated as a three-field problem (fluid, structure, and pseudo-structural dynamic mesh) governed by the following coupled semi-discrete equations [LES 93], [FAR 95b], [PIP 95]:

$$
\begin{aligned}
\frac{d}{dt}(A W) + F^c(W, x, \dot{x}) &= R(W, x), \\
M \frac{d^2 u}{dt^2} + D \frac{du}{dt} + K u &= f^{ext}(W(x, t), x), \qquad [1] \\
\widetilde{M} \frac{d^2 x}{dt^2} + \tilde{D} \frac{dx}{dt} + \widetilde{K} x &= 0,
\end{aligned}
$$

where a dot denotes a time-derivative, x is the displacement or position vector of the moving fluid grid points (depending on the context), W is the fluid state vector, u is the structural displacement vector, M, D, and K denote respectively the finite element mass, damping, and stiffness matrices of the structure, f^{ext} is the vector of external forces acting on the structure, x is the grid displacement vector, $\widetilde{M}$, $\widetilde{D}$, and $\widetilde{K}$ are fictitious mass, damping, and stiffness matrices associated with the moving fluid grid and constructed to control its motion, A results from the finite element/volume discretization of the fluid equations, $F^c = F - \dot{x}W$ is the vector of Arbitrary Lagrangian Eulerian (ALE) convective fluxes, F denotes the vector of convective fluxes and R the vector of diffusive fluxes. The first two equations of [1] express the equilibrium of the fluid and structure subsystems, respectively. The third equation is a mathematical representation of a fluid dynamic mesh (note that $\widetilde{M} = \tilde{D} = 0$ includes as particular cases the spring analogy and continuum mechanics based mesh motion schemes advocated by many investigators [BAT 90], [FAR 98a]).

For complex structural systems, the simultaneous solution of [1] by a monolithic scheme (the three fields are combined in a single numerical formulation) is in general computationally challenging, mathematically and economically suboptimal, and software-wise unmanageable.

Alternatively, equations [1] can be solved by a partitioned procedure where the fluid and structure subproblems are time-discretized by different methods tailored to their different mathematical models, and the resulting discrete equations can be solved by a "staggered", or "segregated", or "time-lagged" algorithm (see for example [FAR 95b], [PIP 95], [STR 90], [MOU 96], [GUP 96]). Such a strategy simplifies explicit/implicit treatment, subcycling, load balancing, software modularity, and soft-

ware replacements as better mathematical models and methods emerge in the fluid and/or structure disciplines. The basic, most popular staggered algorithm, referred to in this paper as the Conventional Serial Staggered (CSS) procedure, goes as follows:

(a) transfer the motion of the wet structural boundary to the fluid system,

(b) update the position of the moving fluid mesh accordingly,

(c) advance the fluid system and compute new pressure and fluid stress fields,

(d) convert the new fluid pressure and stress fields into a structural load,

(e) advance the structural system under the flow induced load.

Such a staggered procedure, which can be described as a loosely coupled solution algorithm, can also be equipped with a subcycling strategy where the fluid and structure subsystems are advanced using different time-steps Δt_F and Δt_S [PIP 95]. Usually, one has $\Delta t_F \leq \Delta t_S$.

Unfortunately, it is well-known that the time-accuracy of the CSS procedure is in general at least one order lower than that of its underlying flow and structure time-integrators, and its stability limit can be much more restrictive than that of the flow and/or structure solvers. For this reason, several ad-hoc strategies have been published in the literature for improving the time-accuracy and stability properties of the CSS procedure. Most of them consist essentially in inserting some type of predictor/corrector iterations within each cycle of the CSS procedure, in order to compensate for the time-lag between the fluid and structure solvers [STR 90], [PRA 94].

The mathematical analysis of the time-accuracy and numerical stability of partitioned procedures constructed for the solution of equations [1] has been at center of many works, including those of the authors, for years. However, because the dependence of the structure equations of equilibrium on the motion of the fluid dynamic mesh is implicit rather than explicit, and the fluid equations of motion can be strongly non-linear, our previous investigations were limited to a one-dimensional aeroelastic model problem [PIP 95]. This analysis yielded guidelines for exchanging aerodynamic and elastodynamic data (possibly in the presence of subcycling) in a manner that preserves the unconditional stability and order of time-accuracy of a given partitioned procedure. We were able to apply some but not all of these ideas to the realistic problem represented by equations [1] [PIP 97]. However, the formal analysis of staggered algorithms remains a formidable challenge, because of the same reasons that previously incited us to consider a representative model problem.

For this reason, we sum up in this paper our previous contributions, including a very promising criterion for assessing the suitability of a given partitioned procedure for the solution of the non-linear transient aeroelastic equations [1], and we give new perspectives for the construction of more efficient partitioned procedures, based on the designed criterion [PIP 99a]. This criterion is essentially based on the evaluation of the energy that is numerically – and hence, artificially – created at the fluid-structure interface by the staggering process and typically dictates the choice of the predictor, and/or the time-discretization of the transfer of the fluid pressure and stress fields to

the structure subsystem. Since it is very effective at discriminating between staggered algorithms as well as improving them, we apply this criterion to the analysis of new partitioned procedures constructed with enhanced parallel features, in the case of two- and three-dimensional, transonic and supersonic, wing and panel flutter problems.

2. An energy-based analysis

The global system defined by the union of the fluid and structure subsystems being a closed system, it follows that at each time t, the reaction of the structure is equal to the action of the fluid and the works performed by the structural forces and by the fluid pressure and stress fields at the fluid-structure interface $\Gamma_{F/S}$ must be opposite.

In [LES 95], [LES 96], [PIP 97], it was argued and shown that the loss in time-accuracy and numerical stability induced by staggering can be traced to a lack of conservation of the momentum and energy at the fluid-structure interface. It was also argued in [PIP 97] that the time-accuracy and stability properties of a given partitioned procedure can be improved by controlling the unbalance of energy at $\Gamma_{F/S}$.

In view of the above remarks, we have proposed a framework for analyzing partitioned procedures designed for the solution of equations [1] that is based on the evaluation of the works performed at the fluid-structure interface. More specifically, given the fluid and structure responses predicted by a staggered algorithm at each time t^n – where n designates the n-th time-station – we propose to evaluate a partition procedure by assessing the order of the difference between the work performed by the fluid pressure and stress fields, and that performed by the structural forces, at the fluid-structure interface, as a function of the computational time-step. Not only such a criterion can discriminate between different partitioned procedures designed for the solution of non-linear transient aeroelastic problems, but it can also suggest a conservative time-discretization of the pressure and stress fields transmitted by the fluid to the structure. A similar idea was exploited in [FAR 98b] to semidiscretize (in space) the exchange of aerodynamic data between the fluid and the structure across non-matching discrete fluid and structure interfaces.

In order to simplify our analysis, we consider only a generic point on the fluid-structure interface, and a surrounding patch of unit length in two dimensions, and unit area in three dimensions. We denote by P the pressure at this point, and consider the case of an inviscid flow. The extension of our analysis to a viscous flow is straightforward. We apply our analysis framework to the investigation of several staggered algorithms: serial or parallel, collocated or non-collocated. Because the aeroelastic structural response is usually dominated by low frequencies, we consider exclusively an implicit structural time-integrator. More specifically, we consider only the mid-point rule because of the popularity of this scheme in production structural codes. Even though for aeroelastic applications we also recommend an implicit scheme as a flow time-integrator, we consider both explicit and implicit flow solvers because of the popularity of both approaches in the computational fluid dynamics community.

2.1. Analysis of serial collocated partitioned procedures

2.1.1. The generalized conventional serial staggered (GCSS) procedure

First, we consider the popular CSS procedure as summarized by Farhat *et al.* [FAR 96]. This partitioned procedure is collocated – that is, it evaluates the fluid and the structure subsystems at the same time-stations. It is serial, or sequential, i.e. the fluid and the structure are advanced in time successively, but not simultaneously.

We generalize this method to incorporate a prediction of the displacement of the structure and an evaluation of the flow induced structural load after the fluid subsystem has been advanced from one time-step to the next one. Each cycle $[t^n, \; t^{n+1}]$ of the GCSS procedure goes as follows:

Step 1. Predicts the structural displacement at time t^{n+1}

$$u^{n+1^p} = u^n + \alpha_0 \Delta t_S \dot{u}^n + \alpha_1 \Delta t_S \left(\dot{u}^n - \dot{u}^{n-1} \right), \qquad [2]$$

where α_0 and α_1 are two real constants. The prediction [2] is first-order time-accurate if $\alpha_0 = 1$, and second-order time-accurate if $\alpha_0 = 1$ and $\alpha_1 = 1/2$. Then, transfers the motion of the wet boundary of the structure to the fluid.

Step 2. Updates the position of the fluid grid x^{n+1} to match on $\Gamma_{F/S}$ the position that the structure would have if it were advanced by the predicted displacement u^{n+1^p}. Then, time-integrates the fluid subsystem from t^n to $t^{n+1} = t^n + \Delta t_S$ using a fluid time-step $\Delta t_F \leq \Delta t_S$. If $\Delta t_F \neq \Delta t_S$, subcycles the flow solver.

Step 3. Transfers a fluid pressure field P_S^{n+1} to the structure, and computes the corresponding flow induced structural load $f_{F/S}^{n+1}$. In the case where the fluid and structure meshes have non-conforming discrete interfaces, a conservative algorithm for computing the spatial distribution of $f_{F/S}^{n+1}$ is recommended [FAR 98b].

Step 4. Time-integrates the structure subsystem from t^n to $t^{n+1} = t^n + \Delta t_S$.

Note that when the flow solver is subcycled, the velocity of the fluid moving grid is held constant constant and equal to $\dot{x} = (x^{n+1} - x^n)/\Delta t_S$, in order to satisfy the geometric conservation law (GCL) [LES 95], [LES 96]. Also, P_S^{n+1} is "a" pressure field sent to the structure and computed after the fluid subsystem has been advanced from t^n to t^{n+1}. Most importantly, P_S^{n+1} *is not necessarily the pressure field P^{n+1} which is computed by the flow solver at time-station t^{n+1}.* Hence, a specific expression of P_S^{n+1} defines a particular instance of the generalized CSS procedure, and can vary from one staggered solution algorithm to another.

2.1.2. Energy balance at the fluid-structure interface

As stated earlier, we assume in this paper that the structural subsystem is always time-integrated by the midpoint rule, but we do not make any assumption for the choice of the flow time-integrator. For any given unsteady flow solver, the energy transferred during the time-interval $[t^n, \; t^{n+1}]$ from the fluid to the structure through

a patch of $\Gamma_{F/S}$ of unit length/area, as viewed by the fluid, can be evaluated as

$$\Delta E_F^{n+1} = - \int_{t^n}^{t^{n+1}} \boldsymbol{f}_F^T(t)\dot{x}(t)dt = -\boldsymbol{P_F}^{n+1^T}\left(x^{n+1} - x^n\right), \qquad [3]$$

where the superscript T designates the transpose operation, $\boldsymbol{f}_F$ denotes the pressure forces exerted by the fluid on $\Gamma_{F/S}$, and $\boldsymbol{P_F}^{n+1}$ is a vector of nodal pressures whose exact expression depends on the time-integrator used by the flow solver. More specifically, $\boldsymbol{P_F}^{n+1}$ depends on the fluid pressure values that are used by the flow solver to compute the fluxes across the interface boundary $\Gamma_{F/S}$, when advancing the fluid state vector from t^n to t^{n+1}. Hence, $\boldsymbol{P_F}^{n+1}$ can take any of the following values

$$\text{explicit forward-Euler scheme:} \qquad \boldsymbol{P_F}^{n+1} = \boldsymbol{P}^n. \qquad [4a]$$

$$\text{implicit backward-Euler scheme:} \qquad \boldsymbol{P_F}^{n+1} \sim \boldsymbol{P}^{n+1}. \qquad [4b]$$

$$\text{second-order time-accurate solvers:} \qquad \boldsymbol{P_F}^{n+1} \sim (\boldsymbol{P}^n + \boldsymbol{P}^{n+1})/2. \qquad [4c]$$

$$\text{subcycling with } \Delta t_F << \Delta t_S: \qquad \boldsymbol{P_F}^{n+1} \sim \frac{1}{\Delta t_S}\int_{t^n}^{t^{n+1}} \boldsymbol{P}(t)dt. \qquad [4d]$$

For one-dimensional aeroelastic problems where the interface $\Gamma_{F/S}$ reduces to a single point, formulas [4] are exact. For two- and three-dimensional problems, we use it to estimate the energy transferred from the fluid to the structure, as viewed by the fluid.

Next, we turn our attention to the energy transferred from the fluid to the structure, as viewed by the structure. First, we note that the displacement, velocity, and acceleration of the structure computed by the midpoint rule satisfy

$$\begin{cases} u^{n+1} = u^n + \Delta t_S(\dot{u}^n + \dot{u}^{n+1})/2, \\ \dot{u}^{n+1} = \dot{u}^n + \Delta t_S(\ddot{u}^n + \ddot{u}^{n+1})/2, \\ M\ddot{u}^{n+1} + D\dot{u}^{n+1} + Ku^{n+1} = P_S^{n+1}. \end{cases} \qquad [5]$$

Hence, if the structural energy is defined as $E_S = \frac{1}{2}\dot{u}^T M\dot{u} + \frac{1}{2}u^T Ku$, it follows from equations [5] that the variation of E_S during a time-step Δt_S is given by

$$E_S^{n+1} - E_S^n = \left(\frac{\boldsymbol{P_S}^n + \boldsymbol{P_S}^{n+1}}{2}\right)^T \left(u^{n+1} - u^n\right) - \Delta t_S \dot{u}^{n+\frac{1}{2}^T} D\dot{u}^{n+\frac{1}{2}}. \qquad [6]$$

The first right hand side term of [6] represents the energy transferred from the fluid to the structure, as viewed by the structure. Hence, this energy can be written as

$$\Delta E_S^{n+1} = \left(\frac{\boldsymbol{P_S}^n + \boldsymbol{P_S}^{n+1}}{2}\right)^T \left(u^{n+1} - u^n\right). \qquad [7]$$

From equations [3] and [7], it follows that the GCSS procedure conserves energy at the fluid-structure interface if and only if $\Delta E_F^{n+1} + \Delta E_S^{n+1} = 0$, i.e.

$$\boldsymbol{P_F}^{n+1^T}\left(x^{n+1} - x^n\right) = \left(\frac{\boldsymbol{P_S}^n + \boldsymbol{P_S}^{n+1}}{2}\right)^T \left(u^{n+1} - u^n\right). \qquad [8]$$

This relationship underscores the importance of formulating computational aeroelasticity problems as *three-field problems* (the fluid, the structure, the fluid dynamic mesh), especially for the analysis of their solution by partitioned procedures.

In general, the predictor [2] – and for that matter any other predictor – does not guess exactly the position of the structure at t^{n+1}; therefore

$$\left(x^{n+1} - x^n\right) \neq \left(u^{n+1} - u^n\right) \quad \text{on} \quad \Gamma_{F/S}. \qquad [9]$$

Furthermore, although $P_S{}^{n+1}$ is a free parameter of the generalized CSS procedure, it cannot be easily constructed to enforce the conservation equation [8], because u^{n+1} is computed by a partitioned procedure only after $P_S{}^{n+1}$ has been evaluated. For all these reasons, we conclude that the general family of collocated partitioned procedures, and more specifically the GCSS procedure, cannot conserve energy at the fluid-structure interface $\Gamma_{F/S}$. However, three key algorithmic components can be carefully adjusted for controlling the unbalance of energy at $\Gamma_{F/S}$, and reducing it as much as possible:

– The motion scheme of the dynamic fluid mesh;

– The structural predictor;

– The time-discretization of the transfer during $[t^n,\ t^{n+1}]$ of the aerodynamic data from the fluid to the structure, i.e. the construction of the pressure field $P_S{}^{n+1}$.

2.1.3. *Framework for characterizing a partitioned procedure*

Here, we specify our framework of analysis and illustrate it for one particular instance of the GCSS procedure. Our objective is to estimate the amount of energy unbalance created at the fluid-structure interface $\Gamma_{F/S}$ by a staggering process during a relatively long period of time. To this end, we make the following assumptions:

– The only external forces applied to the structure are those corresponding to the flow pressure on $\Gamma_{F/S}$;

– The structure is vibrating with a constant amplitude u_0 and circular frequency ω: $u(t) = u_0 \cos(\omega t)$;

– The pressure induced by the flow on $\Gamma_{F/S}$ is also vibrating at the same circular frequency ω, but with a phase difference denoted by φ: $P(t) = P_0 \cos(\omega t + \varphi)$. This phase difference can be linked to well-known added mass, damping, and stiffness effects of a fluid loading. We define two scalar parameters k and d as follows:

$$k = u_0^T P_0 \cos \varphi, \qquad d = u_0^T P_0 \sin \varphi; \qquad [10]$$

– The fluid and structure subsystems are advanced in time using fixed time-steps Δt_F and Δt_S, respectively.

To illustrate our analysis framework, we consider first a specific instance of the GCSS procedure where the prediction step is as trivial as $x^{n+1} = u^{n+1^p} = u^n$

($\alpha_0 = \alpha_1 = 0$), $\boldsymbol{P_S}^{n+1}$ is constructed as $\boldsymbol{P_S}^{n+1} = \boldsymbol{P}^{n+1}$ – i.e. the pressure field sent to the structure is the most recent pressure field computed by the flow solver – and the fluid subsystem is time-integrated by the explicit forward-Euler scheme (which implies $\boldsymbol{P_F}^{n+1} = \boldsymbol{P}^n$), with $\Delta t_F = \Delta t_S = \Delta t$. Let

$$T_\omega = 2\pi/\omega, \quad h = \omega\Delta t. \qquad [11]$$

At each time-step, the structure and fluid variables u^n and $\boldsymbol{P}^n$ computed by this collocated partitioned procedure can be viewed as approximations of $u(t^n)$ and $\boldsymbol{P}(t^n)$, where $t^n = n\Delta t$. From equations [3] and [10], it follows that

$$\Delta E_F^{n+1} = [k\cos(\omega t^n) - d\sin(\omega t^n)]\left(\cos(\omega t^{n-1}) - \cos(\omega t^n)\right). \qquad [12]$$

The energy $\Delta E_F^{NT_\omega}$ transferred during the time-interval $[0, N \times T_\omega]$ from the fluid to the structure through a patch of $\Gamma_{F/S}$ of unit length/area, as viewed by the fluid, can be estimated by summing ΔE_F^n from $n = 0$ to $n = 2N\pi/h = NT_\omega/\Delta t$. Noting that for large values of N/h

$$\begin{cases} \sum_{n=0}^{2N\pi/h} \cos(\omega t^{n-1} + h)\cos(\omega t^{n-1}) & \sim & \frac{N\pi}{h}\cos(h), \\ \sum_{n=0}^{2N\pi/h} \sin(\omega t^{n-1} + h)\sin(\omega t^{n-1}) & \sim & \frac{N\pi}{h}\cos(h), \\ \sum_{n=0}^{2N\pi/h} \sin(\omega t^{n-1} + h)\cos(\omega t^{n-1}) & \sim & \frac{N\pi}{h}\sin(h), \end{cases} \qquad [13]$$

we deduce from equations [12-13] that $\Delta E_F^{NT_\omega} = \sum_{n=0}^{2N\pi/h} \Delta E_F^n \sim N\pi\, \delta E_F$ with $\delta E_F = [k(\cos(h) - 1) - d\sin(h)]/h$. Assuming $h \equiv \omega\Delta t \ll 1$, δE_F can be expressed as $\delta E_F = -d - kh/2 + dh^2/6 + kh^3/24 + O(h^4)$. An estimate of the energy $\Delta E_S^{NT_\omega}$ viewed by the structure can be derived using a similar approach, which leads to $\Delta E_S^{NT_\omega} = \sum_{n=0}^{2N\pi/h} \Delta E_S^n \sim N\pi\, \delta E_S$ with $\delta E_S = d - dh^2/6 + O(h^3)$. From the previous equations, it follows that for the specific collocated partitioned procedure described above, the total energy created artificially at the fluid-structure interface by the staggering process is

$$\Delta E_F^{NT_\omega} + \Delta E_S^{NT_\omega} \sim N\pi\,(\delta E_F + \delta E_S) = N\pi(-k\frac{h}{2} + O(h^2)). \qquad [14]$$

Finally, the parameter $\delta E \equiv \delta E_F + \delta E_S$ is used to assess the accuracy and numerical stability of a partitioned procedure proposed for the solution of equations [1]. For relatively small time-steps ($h \equiv \omega\Delta t \ll 1$), this parameter δE can warn the analyst that his/her chosen partitioned procedure will introduce positive or negative damping in the computed aeroelastic response, depending on the signs and relative magnitudes of k and d (which depend on the distribution of the aerodynamic loads on the structure). This framework of analysis can be applied to many partitioned procedures. We shall say that a partitioned procedure is n^{th}-order energy-accurate if $\delta E \sim C\, h^n$ when $h \to 0$, where C is a constant. Note that the parameters δE_F and δE_S can be estimated separately.

2.1.4. *Evaluation of δE_F for various flow time-integrators*

Here, we consider again the GCSS procedure presented in Section 2.1.1, but equipped with the two-parameter predictor [2], and various schemes for time-integrating the semidiscrete fluid equations (and then various expressions of $P_F{}^{n+1}$). For each case, we give the value of the estimated energy δE_F:

$$\text{forward-Euler [4a]:} \quad \delta E_F = \begin{cases} -d + (\alpha_0 - \frac{1}{2})kh + (\frac{1}{6} - \frac{\alpha_0}{2} + \alpha_1)dh^2 \\ +(\frac{1}{24} - \frac{\alpha_0}{6} + \alpha_1)kh^3 + O(h^4). \end{cases} \quad [15a]$$

$$\text{backward-Euler [4b]:} \quad \delta E_F = \begin{cases} -d + (\alpha_0 - \frac{3}{2})kh + (\frac{7}{6} - \frac{3\alpha_0}{2} + \alpha_1)dh^2 \\ +(\frac{5}{8} - \frac{7\alpha_0}{6} + 2\alpha_1)kh^3 + O(h^4). \end{cases} \quad [15b]$$

$$2^{nd}\text{-order solvers [4c]:} \quad \delta E_F = \begin{cases} -d + (\alpha_0 - 1)kh + (\frac{2}{3} - \alpha_0 + \alpha_1)dh^2 \\ +(\frac{1}{3} - \frac{2\alpha_0}{3} + \frac{3\alpha_1}{2})kh^3 + O(h^4). \end{cases} \quad [15c]$$

$$\text{subcycling [4d]:} \quad \delta E_F = \begin{cases} -d + (\alpha_0 - 1)kh + (\frac{7}{12} - \alpha_0 + \alpha_1)dh^2 \\ +(\frac{1}{4} - \frac{7\alpha_0}{12} + \frac{3\alpha_1}{2})kh^3 + O(h^4). \end{cases} \quad [15d]$$

2.1.5. *Evaluation of δE_S for various choices of $P_S{}^{n+1}$*

Next, we focus on the treatment of the structural equations by the GCSS procedure and we only consider the trapezoidal rule for their time-integration. We use the following formulation, which fits the midpoint rule (rather than the Newmark method with $\beta = 1/4$ and $\gamma = 1/2$)

$$(\frac{4M}{\Delta t_S^2} + \frac{2D}{\Delta t_S} + K)u^{n+1/2} = \frac{P_S{}^n + P_S{}^{n+1}}{2} + (\frac{4M}{\Delta t_S^2} + \frac{2D}{\Delta t_S})u^n + \frac{2M}{\Delta t_S}\dot{u}^n, \quad [16]$$

whose solution determines the displacement $u^{n+1} = 2u^{n+1/2} - u^n$. The reader can refer to [PIP 99b] for a discussion on differences in implementations, whether a Newmark-type or a midpoint rule formulation is used.

We investigate different approaches for constructing a flow induced structural load $P_S{}^{n+1}$ after the fluid subsystem has been advanced from t^n to t^{n+1}. We can consider the four choices $P_S{}^{n+1} = P_F{}^{n+1}$ and the four choices $P_S{}^{n+1/2} = P_F{}^{n+1}$ (with $P_S{}^{n+1/2} = (P_S{}^n + P_S{}^{n+1})/2$), deriving from each possible choice for the flow time-integrator [4]. We give the corresponding value of the estimated energy δE_S:

$$P_S{}^{n+1} = P_F{}^{n+1}[4a]: \quad \delta E_S = d - kh - \frac{2}{3}dh^2 + \frac{1}{3}kh^3 + O(h^4). \quad [17a]$$

$$P_S{}^{n+1} = P_F{}^{n+1}[4b]: \quad \delta E_S = d - \frac{1}{6}dh^2 + O(h^4). \quad [17b]$$

$$P_S{}^{n+1} = P_F{}^{n+1}[4c]: \quad \delta E_S = d - \frac{1}{2}kh - \frac{5}{12}dh^2 + \frac{1}{6}kh^3 + O(h^4). \quad [17c]$$

$$P_S{}^{n+1} = P_F{}^{n+1}[4d]: \quad \delta E_S = d - \frac{1}{2}kh - \frac{1}{3}dh^2 - \frac{1}{8}kh^3 + O(h^4). \quad [17d]$$

$$\boldsymbol{P_S}^{n+1/2} = \boldsymbol{P_F}^{n+1}[4a]: \quad \delta E_S = d - \frac{1}{2}kh - \frac{1}{6}dh^2 + \frac{1}{24}kh^3 + O(h^4). \quad [18a]$$

$$\boldsymbol{P_S}^{n+1/2} = \boldsymbol{P_F}^{n+1}[4b]: \quad \delta E_S = d + \frac{1}{2}kh - \frac{1}{6}dh^2 - \frac{1}{24}kh^3 + O(h^4). \quad [18b]$$

$$\boldsymbol{P_S}^{n+1/2} = \boldsymbol{P_F}^{n+1}[4c]: \quad \delta E_S = d - \frac{1}{6}dh^2 + O(h^4). \quad [18c]$$

$$\boldsymbol{P_S}^{n+1/2} = \boldsymbol{P_F}^{n+1}[4d]: \quad \delta E_S = d - \frac{1}{12}dh^2 + O(h^4). \quad [18d]$$

2.1.6. *Energy analysis of collocated partitioned procedures*

The various flow time-integrators discussed in Section 2.1.4, the different schemes for transmitting the fluid data to the structure exposed in Section 2.1.5, and the various instances of the structural predictor [2] can be combined to generate different family members of the GCSS procedure presented in Section 2.1.1. For each resulting partitioned procedure, the corresponding expression of the energy $\delta E = \delta E_F + \delta E_S$ can be obtained by combining the results of Section 2.1.4 and Section 2.1.5, and specifying the values of α_0 and α_1 in the predictor [2]. Here, we summarize the energy analysis of these collocated partitioned procedures.

* Trivial prediction. First, we consider the case where $\alpha_0 = \alpha_1 = 0$, i.e. $\boldsymbol{u}^{n+1^P} = \boldsymbol{u}^n$. The reader can check that such a predictor always lead to a first-order energy-accurate CSS method, except in one instance. When the fluid subsystem is time-integrated by a first-order explicit scheme ($\Rightarrow \boldsymbol{P_F}^{n+1} = \boldsymbol{P}^n$) and $\boldsymbol{P_S}^{n+1/2} = \boldsymbol{P}^{n+1}$, the resulting CSS partitioned procedure becomes at least fourth-order energy-accurate. However, this specific instance of the CSS method does not conserve well the momentum at the fluid-structure interface (momentum variations of the fluid and the structure during a time-step are not accurately opposite), and becomes less energy-accurate when the fluid system is subcycled.

* First-order prediction. Next, we consider the first-order prediction obtained by setting $\alpha_0 = 1$ and $\alpha_1 = 0$ in [2]. In that case, several CSS algorithms become second-order energy-accurate. The optimal one (using a second-order time-accurate flow integrator and $\boldsymbol{P_S}^{n+1}$ given by [18d] is such that $\delta E = -5dh^2/12 + O(h^3)$.

* Second-order prediction. The second-order prediction of the structural displacement obtained with $\alpha_0 = 1$ and $\alpha_1 = 1/2$ leads to third-order energy-accurate CSS procedures if and only if $\boldsymbol{P_S}^{n+1/2} = \boldsymbol{P_F}^{n+1}$, where $\boldsymbol{P_F}^{n+1}$ depends on the flow time-integrator [18a-18d]. Independently of the flow time-integrator, momentum is conserved at $\Gamma_{F/S}$ (momentum variations of the fluid and the structure during a time-step are numerically opposite) and $\delta E = 5kh^3/12 + O(h^4)$.

2.2. *Analysis of a serial non-collocated partitioned procedure*

In [LES 95], [LES 96], [FAR 96], [LES 98], Lesoinne and Farhat have shown that collocated partitioned procedures can never satisfy simultaneously both displacements and velocities continuity equations on the fluid-structure interface, while verifying the Geometrical Conservation Law (GCL) in the fluid domain [THO 79], [LES 95], [LES 96]. Because of staggering, continuity of displacements at $\Gamma_{F/S}$ is almost never satisfied. Also, the continuity of velocities at $\Gamma_{F/S}$, the satisfaction of the GCL, and the use of the trapezoidal rule for the structure are incompatible.

Given that both continuity equations are desirable in order not to introduce any parasitic discontinuity at $\Gamma_{F/S}$ where the interaction between the fluid and the structure occurs, and violating the GCL restricts severely the time-step of the flow-integrator and/or the coupling time-step Δt_S [FAR 95b], [GUI 99], Lesoinne and Farhat have proposed to resolve this dilemma by non-collocating the staggered procedure. Their advocated algorithm, named the Improved Serial Staggered (ISS) procedure, is built as a leap-frog scheme (and then it is basically sequential) where the fluid subsystem is always computed at half time-stations $(\cdots, t^{n-\frac{1}{2}}, t^{n+\frac{1}{2}}, t^{n+\frac{3}{2}}, \cdots)$, while the structure subsystem is always computed at full time-stations $(\cdots, t^n, t^{n+1}, t^{n+2}, \cdots)$. The ISS staggered procedure can be summarized as follows [LES 98]:

– Predicts the structural displacement at time $t^{n+\frac{1}{2}}$: $u^{n+\frac{1}{2}^p} = u^n + \frac{\Delta t_S}{2} \dot{u}^n$;

– Updates the position of the fluid grid $x^{n+\frac{1}{2}}$ to match on $\Gamma_{F/S}$ the predicted position $u^{n+\frac{1}{2}^p}$. Then, time-integrates the fluid subsystem from $t^{n-\frac{1}{2}}$ to $t^{n+\frac{1}{2}} = t^{n-\frac{1}{2}} + \Delta t_S$ using a fluid time-step $\Delta t_F \leq \Delta t_S$. If $\Delta t_F \neq \Delta t_S$, subcycles the flow solver;

– Transfers a fluid pressure field P_S^{n+1} to the structure, and computes the corresponding flow induced structural load $f_{F/S}^{n+1}$. Then, time-integrates the structure subsystem from t^n to $t^{n+1} = t^n + \Delta t_S$ using the midpoint rule.

Using this non-collocated partitioned method, the expression of the energy ΔE_F transferred during the time-interval $[t^n, t^{n+1}]$ from the fluid to the structure through a patch of $\Gamma_{F/S}$ of unit length/area, as viewed by the fluid, has to be re-adjusted, because unlike the structural subsystem, the fluid subsystem is advanced from $t^{n-\frac{1}{2}}$ to $t^{n+\frac{1}{2}}$). ΔE_F can be computed as

$$[\Delta E_F]_n^{n+1} = [\Delta E_F]_n^{n+\frac{1}{2}} + [\Delta E_F]_{n+\frac{1}{2}}^{n+1} = \frac{1}{2}[\Delta E_F]_{n-\frac{1}{2}}^{n+\frac{1}{2}} + \frac{1}{2}[\Delta E_F]_{n+\frac{1}{2}}^{n+\frac{3}{2}}$$

$$= -\frac{1}{2} P_F^{n+\frac{1}{2}^T}(x^{n+\frac{1}{2}} - x^{n-\frac{1}{2}}) - \frac{1}{2} P_F^{n+\frac{3}{2}^T}(x^{n+\frac{3}{2}} - x^{n+\frac{1}{2}}). \quad [19]$$

Depending on the flow solver with which the ISS procedure is equipped, $P_F^{n+\frac{1}{2}}$ can take several values corresponding to a forward-Euler, backward-Euler, second-order implicit, and highly subcycled flow time-integrator, respectively. The value for δE_F can be computed accordingly. Depending on analogous choices for P_S^{n+1}, es-

timates for δE_S can be obtained, as in [17-refDESB]. From tedious developments on δE for many combinations, we obtain that

* **Second-order energy-accurate** instances of the ISS procedure can be obtained using a flow time-integrator where $\boldsymbol{P_F}^{n+\frac{1}{2}} = \boldsymbol{P}^{n-\frac{1}{2}}$, and setting $\boldsymbol{P_S}^{n+1/2}$ to any of the possible pressure fields deriving from the fluid solvers considered, or using a subcycled flow time-integrator and setting $\boldsymbol{P_S}^{n+1/2} = \boldsymbol{P}^{n+\frac{1}{2}}$. In the latter case, δE becomes $\delta E = -dh^2/12 + O(h^3)$.

* **A third-order energy-accurate** instance of the ISS method can be obtained by choosing a flow time-integrator where $\boldsymbol{P_F}^{n+\frac{1}{2}} = (\boldsymbol{P}^{n-\frac{1}{2}} + \boldsymbol{P}^{n+\frac{1}{2}})/2$ (even when the flow solver is significantly subcycled), and setting $\boldsymbol{P_S}^{n+1/2} = \boldsymbol{P}^{n+\frac{1}{2}}$. This corresponds to the original ISS procedure proposed by Lesoinne and Farhat in [LES 95], [LES 96], [FAR 96], [LES 98]

2.3. *Construction of new serial partitioned procedures*

The analysis presented in this paper gives us the basic tools to construct new partitioned procedures. We can get through many combinations of fluid and structural solvers, as well as choices for the structural predictor and fluid pressure fields transmitted. We have already noticed in Section 2.1.6 that, if a predictor [2] with $\alpha_0 = 1$ and $\alpha_1 = 1/2$ is used and if we set $\boldsymbol{P_S}^{n+1/2} = \boldsymbol{P_F}^{n+1}$, where $\boldsymbol{P_F}^{n+1}$ depends on the flow time-integrator, then the partitioned procedure obtained is **third-order energy-accurate** with $\delta E = 5kh^3/12 + O(h^4)$, independently of the flow time-integrator. Our analysis tells us also, after tedious calculations that

* if a predictor [2] with $\alpha_0 = 3/2$ and $\alpha_1 = 5/4$ is used, whereas $\boldsymbol{P_S}^{n+1} = \boldsymbol{P_F}^{n+1}$, where $\boldsymbol{P_F}^{n+1}$ depends on the flow time-integrator, then the partitioned procedure obtained is again **third-order energy-accurate** with $\delta E = 33kh^3/24 + O(h^4)$, independently of the flow time-integrator.

* finally, a linear combination of the results reported above yields the amazing result that: if a predictor [2] with $\alpha_0 = 18/23$ and $\alpha_1 = 4/23$ is used and if we set $\boldsymbol{P_S}^{n+1} = \frac{56}{23}\boldsymbol{P_F}^{n+1} - \frac{33}{23}\boldsymbol{P_S}^n$, where $\boldsymbol{P_F}^{n+1}$ depends on the flow time-integrator, then the partitioned procedure obtained is **at least fourth-order energy-accurate** ($\delta E = O(h^4)$), independently of the flow time-integrator.

However, the last two families of partitioned procedures do not satisfy one of the most important properties of procedures of the first family mentioned above, which is the conservative exchange of momentum between the fluid and the structure subsystems at each time-step. This momentum unbalance, although the energy error accumulated at the fluid-structure interface is controlled and small, can lead in some undamped cases to high-frequency numerical instabilities (errors in the structural prediction and in momentum conservation are both present).

2.4. *Construction of parallel collocated partitioned procedures*

The collocated and non-collocated partitioned procedures presented in Sections 2.1, 2.2 and 2.3 were all constructed as serial partitioned procedures, in the sense that the fluid and structural subsystems have to be advanced in time successively, and not simultaneously at each coupled time-step. More precisely, the fluid time-integration or the structural time-integration requires an information (coming from the other subsystem) which is not available at the beginning of the coupled time-step.

In this section, we propose new partitioned procedures for the transient solution of the aeroelastic problem [1], which are inherently parallel, i.e. the fluid and the structure can be time-integrated simultaneously inside each coupled time-step. Such procedures can reduce the total simulation time when the computational cost of the structural analyzer is comparable to that of the fluid one, for example, when the structure is a complete aircraft configuration and geometrical non-linearities must be accounted for.

2.4.1. *A new family of parallel partitioned procedures deriving form the GCSS*

We first propose the following parallel version of the GCSS procedure, which can be sketched as

Fluid Step 1. Predicts the structural displacement at time t^{n+1} using formula [2]. Note that this prediction does not require any further structural information than those already known and exchanged before the beginning of the current coupled time-step.

Fluid Step 2. Updates the position of the fluid grid x^{n+1} to match on $\Gamma_{F/S}$ the position that the structure would have if it were advanced by the predicted displacement u^{n+1^p}. Then, time-integrates the fluid subsystem from t^n to t^{n+1} using a fluid time-step $\Delta t_F \leq \Delta t_S$. If $\Delta t_F \neq \Delta t_S$, subcycles the flow solver.

Structural Step 1. Computes a fluid pressure field P_S^{n+1}, depending only on the available fluid field history on $[t^{n-1}, t^n]$, and computes the corresponding flow induced structural load.

Structural Step 2. Time-integrates the structure subsystem from t^n to t^{n+1}.

Note that this procedure is actually parallel, in the sense that fluid and structural steps can be performed simultaneously, and therefore computational load balancing can be done on all fluid and structural subdomains. For this particular partitioned procedure, the energy based analysis leads to the following general results: in the family of parallel partitioned procedures defined above, third-order and even fourth-order energy accurate procedures can be constructed. More precisely,

* if a predictor [2] with $\alpha_0 = \alpha_1 = 2$ is used and if we set $P_S^{n+1/2} = P_F^n$, where P_F^n depends on the flow time-integrator, then the partitioned procedure obtained is **third-order energy-accurate** with $\delta E = 7kh^3/3 + O(h^4)$, independently of the flow time-integrator.

* if a predictor [2] with $\alpha_0 = 5/2$ and $\alpha_1 = 13/4$ is used and if we set $P_S^{n+1} = P_F^n$, where P_F^n depends on the flow time-integrator, then the partitioned procedure obtain-

ed is again **third-order energy-accurate** with $\delta E = 109kh^3/24 + O(h^4)$, independently of the flow time-integrator.

* finally, a linear combination of the results reported above yields the amazing result that if a predictor [2] with $\alpha_0 = 246/109$ and $\alpha_1 = 288/109$ is used and if we set $\boldsymbol{P_S}^{n+1} = \frac{162}{109}\boldsymbol{P_F}^n - \frac{53}{109}\boldsymbol{P_S}^n$, where $\boldsymbol{P_F}^n$ depends on the flow time-integrator, then the partitioned procedure is **at least fourth-order energy-accurate** ($\delta E = O(h^4)$), independently of the flow time-integrator.

Again, this spectacular result tells us that accumulation of artificial energy, created at the fluid-structure interface, can be very well controlled. However, some high-frequency instabilities can appear in partitioned procedures, because of important but compensating errors in momentum conservation and in the structural prediction.

2.4.2. *Other parallel partitioned procedures*

In the previous section, we have shown how to construct families of parallel partitioned procedures, which are quite general, because the coupling algorithm can be designed such that its energy accuracy is independent of the fluid flow solver chosen. However, many more parallel partitioned procedures can be constructed, which are actually third-order energy-accurate for a second-order backward difference scheme flow solver.

Among dozens of third-order energy-accurate partitioned procedures, let us cite the particular instance of the parallel procedure described in the previous section, with $\alpha_0 = 3/2$ and $\boldsymbol{P_S}^{n+1/2} = \boldsymbol{P}^n$. Note that, for this procedure, the fluid pressure field and the corresponding flow induced structural load are not directly derived from $\boldsymbol{P_F}^n$. The energy based analysis leads to the following results: if $\alpha_1 = 1$, then the procedure is third-order energy-accurate with $\delta E = 7kh^3/8 + O(h^4)$; if $\alpha_1 = 5/12$, then the procedure is second-order energy-accurate with $\delta E = -7dh^2/12 + O(h^4)$. Numerical tests involving these procedures will be presented in the sequel.

3. Applications and numerical results

We present here some numerical validation of our energy-based criterion, and in particular of the underlying assumptions stated in Section 2.1.2 and Section 2.1.3. We consider the simulation of the non-linear transient aeroelastic response of two structures: a flat panel with infinite aspect ratio in a critical supersonic air stream in two space dimensions, and the AGARD Wing 445.6 in a transonic air stream in three space dimensions. The complete flutter analysis of both of these problems using collocated and non-collocated partitioned procedures can be found, among others, in [FAR 95a], [FAR 96], [LES 98]. Here, we focus on demonstrating the validity of the energy-based analysis presented herein and its ability to predict and explain the behavior of different partitioned procedures designed for the solution of the three-way coupled fluid-structure equations [1].

For this purpose, we employ a finite element structural code equipped with the midpoint rule as a time-integrator, an unsteady flow solver that operates on unstructured dynamic meshes (the main features are described in [PIP 99b]: second-order spatial accuracy based on MUSCL interpolations [VAN 79], ALE formulation [FAR 95b], several possible time-integrators including a second-order backward difference implicit algorithm that obeys the second-order discrete GCL [KOO 98], [KOO 99]), a "matcher" algorithm [MAM 86] for addressing the geometric issues associated with non-matching fluid and structure meshes, and the conservative method developed in [FAR 98b] for semidiscretizing (in space) the exchange of aerodynamic and elastodynamic data across non-matching fluid and structure discrete interfaces.

3.1. *Supersonic panel flutter*

We first consider the transient aeroelastic response of a clamped flat panel (length $L = 0.5m$, uniform thickness $H = 1.35mm$, Young modulus $E = 7.728 10^{10} N/m^2$, Poisson ratio $\nu = 0.33$, density $\rho_S = 2710 Kg/m^3$) with infinite aspect ratio in a two-dimensional supersonic inviscid air flow [BIS 57], [FAR 95b]. The upper side of the panel is exposed to an air stream ($P_\infty = 25714 \, Pa$, $\rho_\infty = 0.4 \, Kg \, m^{-3}$, supersonic free-stream Mach number M_∞ specified below), and its lower side to still air at a pressure equal to the free-stream pressure P_∞.

The analytical solution of the instability problem of this flat panel can be found under some simplifying assumptions. The critical free-stream Mach number M_∞^{cr}, i.e. the lowest free-stream Mach number for which an unstable aeroelastic mode of the panel appears, is $M_\infty^{cr} = 2.27$ in the present case, with a critical circular frequency $\omega^{cr} = 462 \, rad/s$. Because we are interested in simulating the aeroelastic response of the panel at or near the flutter point, we set the parameters k and d defined in [10] to those obtained for the critical circular frequency ω^{cr}, and the flutter mode U^{cr} (transverse displacement). Here, d is negative, and, because of discretization errors and approximations in the aerodynamic theory, k (which should be zero) is a small *negative* number.

In our numerical simulations, we assume the flow to be inviscid, and impose a slip boundary condition at the fluid-structure interface $\Gamma_{F/S}$. We discretize the flow domain above the panel by 2936 triangles.

First, we perform a reference computation using a very small time-step corresponding to $h = 5.5 \times 10^{-4}$. This simulation predicts a critical free-stream Mach number $M_\infty^{cr} = 2.23$, which is in excellent agreement with the result of the simplified theory ($M_\infty^{cr} = 2.27$). Hence, we set in the sequel the free-stream Mach number to $M_\infty = 2.23$. Next, we consider the simulation by different instances of the GCSS procedure of the aeroelastic response of the panel to an initial perturbation. In all cases, we set Δt_F to a value corresponding to $h = 0.09$ and a subcycling factor $n_{S/F} = (\Delta t_S / \Delta t_F) = 161$. The various instances of the GCSS procedure we con-

sider have in common the same expression for $P_F{}^{n+1}$ [4d] and the same choice for $P_S{}^{n+1/2} = P_F{}^{n+1}$. Hence, these instances of the GCSS method differ only in the selection of the predictor coefficient α_1 in [2] ($\alpha_0 = 1$). The artificially created energy δE for the partitioned procedures considered here can be written as

$$\delta E = d \left(\alpha_1 - \frac{1}{2} \right) h^2 + k \frac{3}{2} \left(\alpha_1 - \frac{2}{9} \right) h^3 + O(h^4). \qquad [20]$$

We report in Figure 1 the obtained computational results for the second modal coordinate of the structural displacement. For $\alpha_1 = 1/2$, δE in [20] is much smaller than for any other value of α_1, which is in agreement with the fact that the numerical simulation performed with $\alpha_1 = 1/2$ reproduces the reference solution. For $\alpha_1 > 1/2$, the leading term in δE is negative because d is negative, which suggests that the partitioned procedure will artificially damp the system. This is confirmed in Figure 1 where the result corresponding to $\alpha_1 = 1$ is reported to be damped. On the other hand, for $\alpha_1 < 1/2$, the leading term in δE is positive, which suggests that the partitioned procedure will artificially feed energy into the system. Again, this is also confirmed in Figure 1 where the result corresponding to $\alpha_1 = -1/2$ suggests that the fluid is feeding energy to the structure.
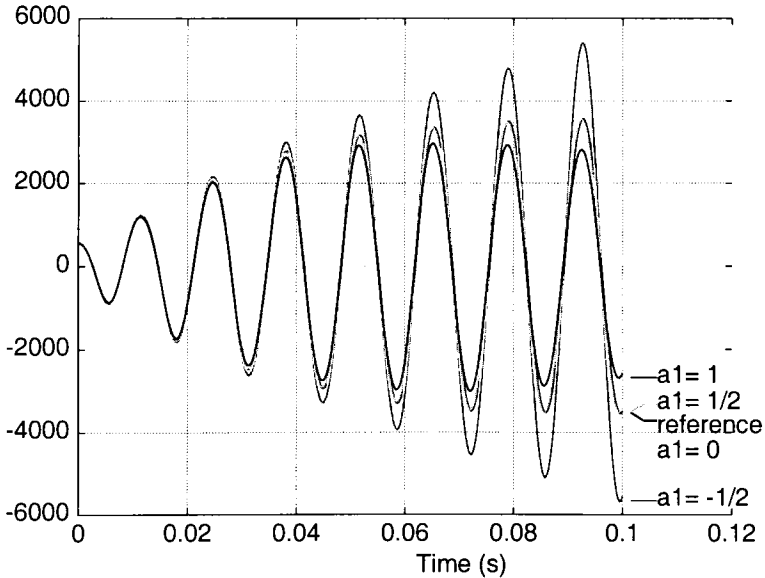
Figure 1. *Computed Second Modal Coordinate ($n_{S/F} = 161$, several α_1)*

In order to highlight the effect on the numerical properties of a partitioned procedure of the choice of the transferred pressure field $P_S{}^{n+1}$, we perform an additional simulation using $\alpha_1 = 1/2$ and the same elements as before, but now with the *standard averaged* pressure field $P_S{}^{n+1} = P_F{}^{n+1}$. We report in Figure 2 the result

generated by this simulation, and contrast it with those of the reference solution, and the simulation performed with the same parameters but with the *improved averaged* pressure field $P_S^{n+1/2} = P_F^{n+1}$. These results reveal a dramatic effect on accuracy (both phase and amplitude of the response) of the choice of P_S^{n+1}. This conclusion is also predicted by our energy-based criterion. Indeed, the change on P_S^{n+1} replaced $\delta E = k\frac{5h^3}{12} + O(h^4)$ by $\delta E = -k\frac{h}{2} - d\frac{h^2}{4} + O(h^3)$, which is almost 150 times larger than the former one (for $h = 0.09$).
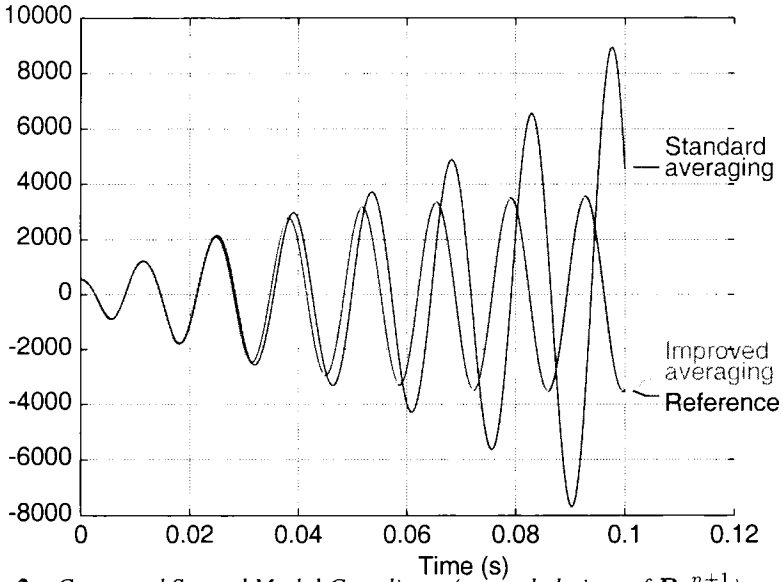
Figure 2. *Computed Second Modal Coordinate (several choices of P_S^{n+1})*

In order to show the different properties of partitioned procedures, including parallel ones, and their effects on the numerical results, we perform other series of simulations with $M_\infty = 1.9$. In that configuration and with this free-stream Mach number, the panel is far from flutter. We set $h = 0.045s$ and we use an implicit backward Euler flow solver and no subcycling ($n_{S/F} = 1$). We perform a series of numerical simulations using the non-collocated ISS method (equipped with $P_S^{n+1/2} = P^{n+\frac{1}{2}}$), for which our analysis predicts $\delta E \sim -kh/2$, and three different instances of the GCSS procedure:

* a Conventional Parallel Staggered (CPS) procedure [FAR 96] with $\alpha_0 = \alpha_1 = 0$, and the pressure field transferred to the structure is chosen as $P_S^{n+1} = P^n$, for which our analysis predicts $\delta E \sim -2kh$.

* another procedure named here CSS1, which differs for the CPS procedure above only by the use of $P_S^{n+1} = P^{n+1}$, for which $\delta E \sim -3kh/2$.

* another procedure denoted by CSS2, which differs from CSS1 by the use of a first-order structural predictor ($\alpha_0 = 1$, $\alpha_1 = 0$), for which $\delta E \sim -kh/2$.

Given that for this problem k is a small negative number, the expressions of δE given above suggest that all four partitioned methods will artificially feed energy into the aeroelastic system, but CSS2 and ISS will inject a smaller numerical energy than the others. This is confirmed by the lift histories simulated by the above partitioned procedures reported in Figure 3. For this problem, the staggered algorithms CPS and CSS1 predict erroneously flutter. The partitioned procedure CSS2 and the ISS method deliver the same accuracy and predict correctly a stable behavior of the panel; however, they exhibit amplitude and phase errors after five periods. This demonstrates once again the ability of our energy-based criterion to predict and explain the behavior of different partitioned procedures designed for the solution of three-way coupled fluid-structure problems.

Dimensional Lift
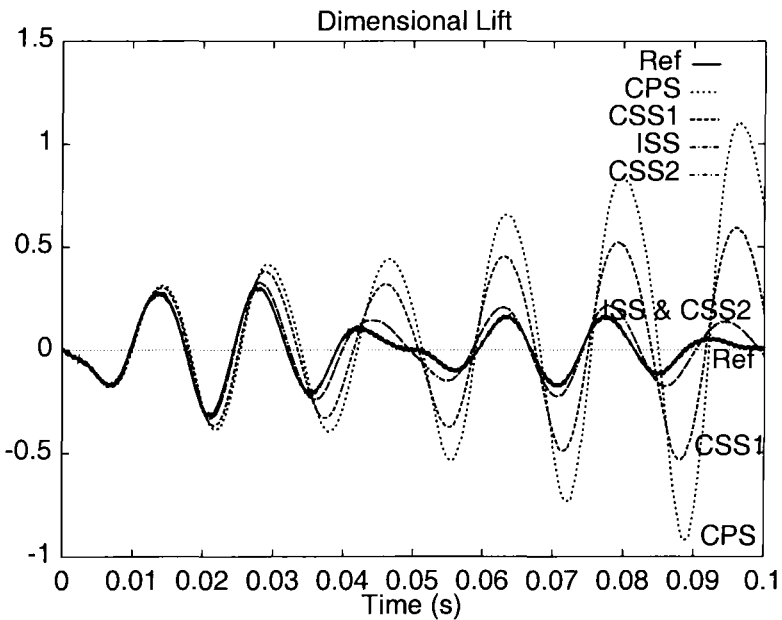
Figure 3. *Lift Histories for Several Serial Procedures*

Finally, we perform a last series of simulations aimed at investigating the possibility to construct accurate and efficient parallel partitioned procedures, like those described in Section 2.4. We now set $h = 0.09s$ and we use an implicit second-order time-accurate flow solver and no subcycling. We compare the serial non-collocated ISS method (equipped with $P_S^{n+1/2} = P^{n+\frac{1}{2}}$ and for a second-order flow solver, we have $\delta E \sim -kh^3/24$) and the two parallel instances of the GCSS procedure presented in Section 2.4.2. As predicted by our energy criterion, the lift histories simulated by the above partitioned procedures reported in Figure 4 show that parallel partitioned procedures can be built to be as accurate and efficient as the most accurate and efficient serial partitioned procedures.
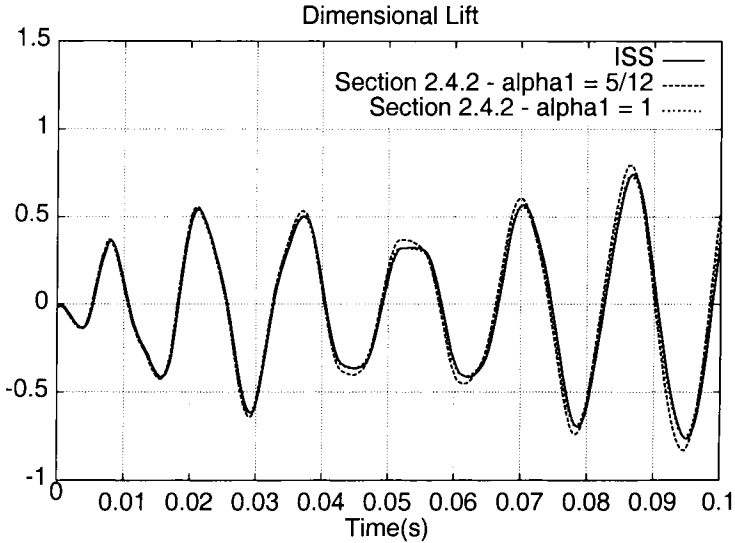
Figure 4. *Lift Histories for Several Parallel Procedures*

3.2. *Flutter analysis of the AGARD Wing 445.6*

We consider now the flutter analysis of the AGARD Wing 445.6 [YAT 87]. The model selected here is the so-called 2.5-ft weakened model 3 whose measured modal frequencies and wind-tunnel flutter test results are reported in [YAT 87], and for which computational aeroelastic data can be found in [LEE 93], [LES 98]. We construct an undamped finite element model of the wing using 800 triangular composite shell elements, which yields 2646 structural degrees of freedom. We generate a three-dimensional unstructured tetrahedral CFD Euler mesh with 22014 vertices (see Figure 5). We set the free-stream conditions to $M_\infty = 0.901$, $\rho_\infty = 1.117 \, 10^{-7}$ slugs/in^3, and $p_\infty = 10$ slugs/(sec$^2 \times$ in). At these flow conditions, the AGARD Wing 445.6 is far from the flutter point. We perturb the wing along its first bending mode, compute a steady-state solution around the deformed configuration of the wing, and then simulate the aeroelastic response to that perturbation using the following partitioned procedures (all equipped with a second-order backward difference implicit scheme that obeys the second-order discrete GCL [KOO 98, KOO 99]):

* the "ISS" (sequential) non-collocated method with $\boldsymbol{P_S}^{n+1/2} = \boldsymbol{P}^{n+\frac{1}{2}}$, for which our analysis predicts $\delta E \simeq -k\frac{h^3}{24}$ (third-order energy-accuracy);

* the instance denoted by "CPS" of the parallel procedure with $\alpha_0 = \alpha_1 = 0$ and $\boldsymbol{P_S}^{n+1} = \boldsymbol{P}^n$, for which $\delta E \simeq -k\frac{3h}{2}$ (first-order energy-accuracy);

* the instance denoted by "CSS1" of the GCSS procedure with $\alpha_0 = \alpha_1 = 0$ and $\boldsymbol{P_S}^{n+1} = \boldsymbol{P}^{n+1}$, for which $\delta E \simeq -kh$ (first-order energy-accuracy);
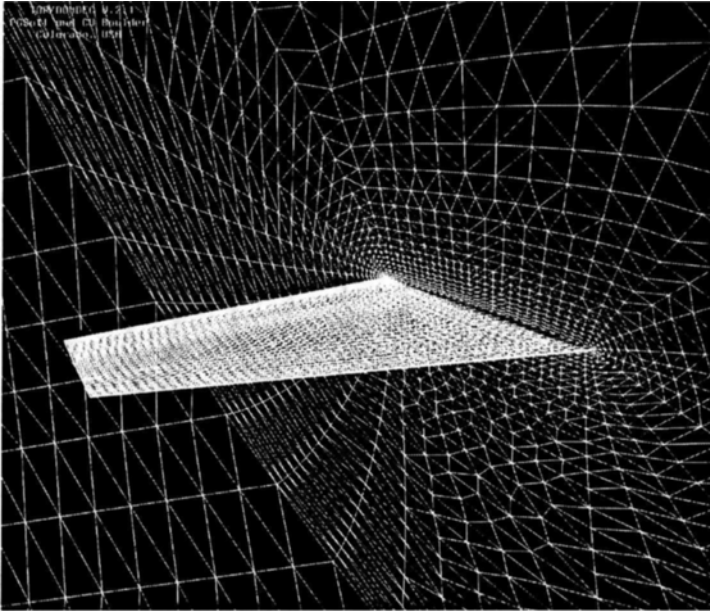
Figure 5. *Partial View of the CFD Mesh for the AGARG Wing 445.6*

Hence, for reasonable time-steps, it can be expected that the ISS method will not introduce or extract a significant amount of numerical energy in or from the system, while the CPS and CSS1 methods will do so. Figure 6 contrasts the lift histories computed by the ISS and CPS methods using various time-steps. For $\Delta t_S = 0.001s$ and $n_{S/F} = 2$, the ISS method is converged in time and predicts a correct stable behavior of the wing. However, for these values of Δt_S and $n_{S/F}$, the CPS method predicts erroneously flutter. This is consistent with the result of our energy-based analysis which shows that the CPS method is only first-order energy-accurate. It takes reducing by one order of magnitude the coupling time-step to $\Delta t_S = 0.0001s$ while maintaining $n_{S/F} = 2$ to get the CPS method to produce the correct solution.

Figure 7 contrasts the lift histories computed by the ISS and CSS1 methods using various coupling time-steps. For $\Delta t_S = 0.001s$ and $n_{S/F} = 2$, the CSS1 method also predicts erroneously flutter. Again, this is consistent with the result of our energy-based analysis which states that the CSS1 method is only first-order energy-accurate. After reducing by a factor equal to five the coupling time-step to $\Delta t_S = 0.0002s$ while maintaining $n_{S/F} = 2$, the CPS method reproduces the same solution as the ISS method.

Again, we perform a second series of simulations with the parallel partitioned procedures described in Section 2.4. We now set $\Delta t_S = 0.0005s$ and no subcycling. We compare the serial non-collocated ISS method (equipped with $\boldsymbol{P_S}^{n+1/2} = \boldsymbol{P}^{n+\frac{1}{2}}$ and for a second-order flow solver, we have $\delta E \sim -kh^3/24$) and the last two parallel in-

stances of the GCSS procedure presented in Section 2.4.2. The lift histories simulated by the above partitioned procedures are reported on Figure 8. Numerical oscillations appear, after a long transient phase. This probably means that our energy criterion is partially correct (since the average curves have a correct reference form) and also that the parallel procedures are slightly unstable. Indeed, the oscillations are amplifying during the whole computation, and the computation stops (too large displacements). The instability is probably due to the lack of momentum conservation at the fluid-structure interface, *and* to the error in the structural prediction. We say "and", because our energy analysis predicts these two errors should compensate.
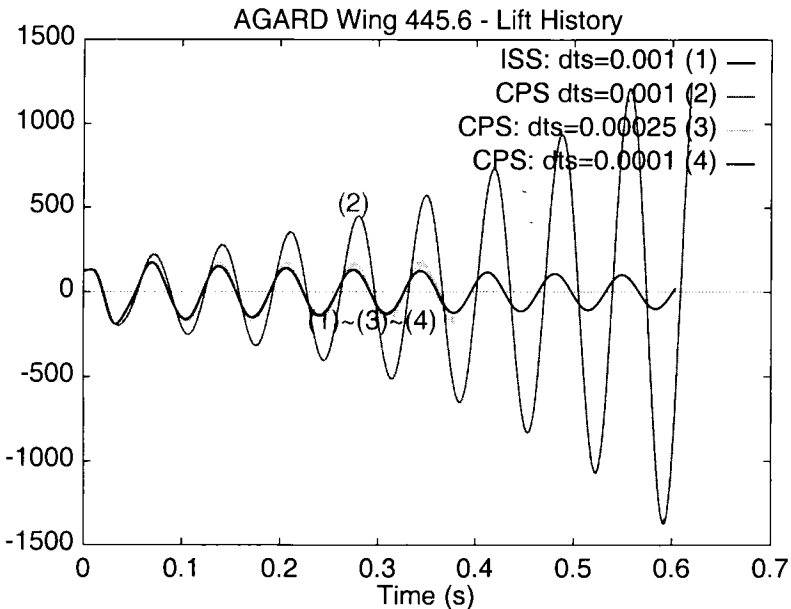
Figure 6. *Lift histories predicted by the ISS and CPS methods*

4. Conclusion

Partitioned procedures are often the method of choice for solving complex multi-disciplinary problems. The governing coupled differential equations are divided into computational groups – called partitions – that are discretized by methods tailored to the underlying mathematical models and geometric complexity. Partitions are advanced with their own time-step and in a staggered fashion, and exchange information at synchronization points only. This strategy simplifies explicit/implicit treatment, sub-cycling, load balancing, software modularity, and replacements as better mathematical models and solution methods emerge in individual disciplines.
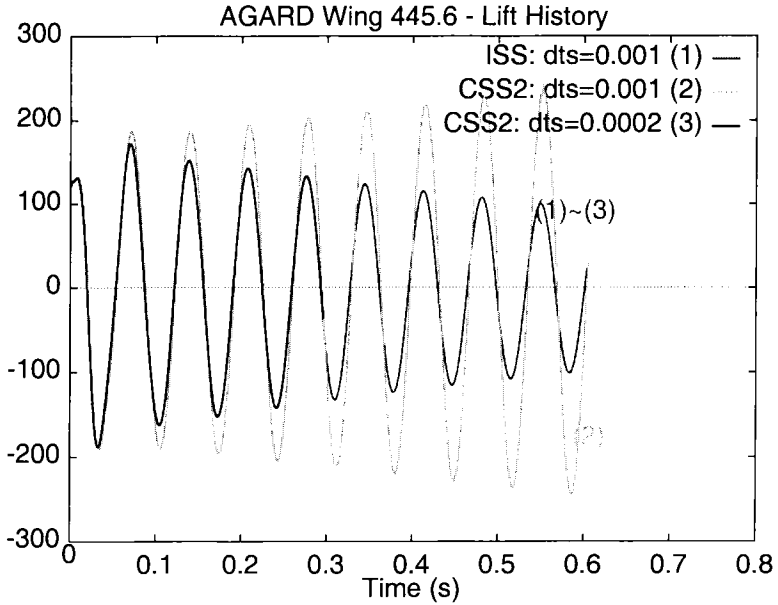
Figure 7. *Lift Histories Predicted by the ISS and CSS1 Methods*
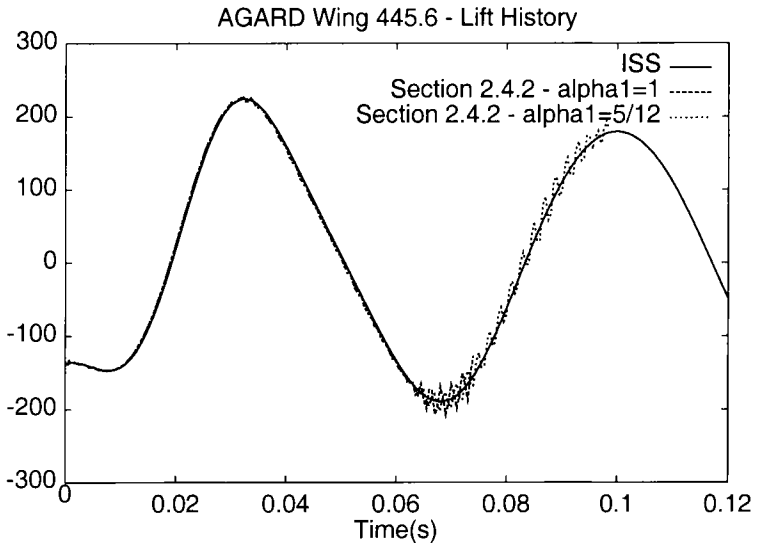
Figure 8. *Lift Histories for Several Parallel Procedures*

However, partitioned procedures are most interesting when they are also computationally efficient, i.e. when they can operate at reasonable time-steps. Staggering is the main reason for restrictive time-steps, but compensating factors such as prediction and improved external vector inputs can be invoked to ensure more reasonable, and sometimes large, time-steps. Understanding the effects of compensating factors is essential for designing computationally efficient staggered algorithms, and is usually achieved by analyzing the numerical properties of a given partitioned procedure.

In this paper, we have focused exclusively on partitioned procedures for the solution of the three-way coupled equations of motion [1] governing non-linear transient aeroelastic problems. We have proposed an analysis framework that is based on the estimation of the energy artificially introduced at the fluid-structure interface by the staggering process. Indeed, the global system defined by the union of the fluid and structure subsystems being a closed one, momentum and energy should be conserved at the fluid-structure interface $\Gamma_{F/S}$. We have introduced the concept of an nth-order energy-accurate partitioned procedure and have proposed a method for evaluating the order of energy-accuracy of any given partitioned method. We advocate the use of this concept for assessing the numerical properties of a given partitioned procedure, and predicting its performance for realistic applications. An energy based criterion is justified by the fact that one of the most important aspects of aeroelastic computations is the prediction of the positive, zero, or negative damping of a given structure by the surrounding flow. Hence, for such problems, it is crucial to select a solution method that is as globally conservative as possible, in order not to contaminate the physical damping by a significant amount of positive or negative artificial numerical damping. We have validated our framework of analysis with the investigation of several partitioned procedures applied to the solution of realistic two- and three-dimensional flutter problems. In each case, we have shown that the higher-order energy-accurate a partitioned procedure is, the more time-accurate it is for a given time-step, and the more computationally efficient it is – that is, the higher is the time-step it affords for a specified accuracy.

We have also shown that our criterion could be used to construct both serial and parallel partitioned procedures with an energy-accuracy up to the fourth order. However, we have noticed that some of these new procedures, and particularly those which are parallel, could lead to numerical, high-frequency instabilities. These results are not completely satisfying, since we would like our criterion to be as general and correctly discriminating as possible. On this subject, the conservation (in the sense of correct exchanges between the fluid and the structure through a coupled time-step) of *both* the momentum and the energy seems to be of great importance. More precisely, our criterion seems to be always correctly discriminating the accurate from the inaccurate partitioned procedures whenever some momentum conservation is enforced at the interface or whenever the structural predictor is accurate enough. For example, it is clear that both predictors of the parallel partitioned procedures presented in Section 2.4.2 are not very accurate. Probably, the use of an inaccurate predictor produces a time shift in the transient behavior of the fluid – this was already noticed in [PIP 96] – which

makes the coefficients k and d in [10] depend on h, and the results of our framework of analysis become inaccurate.

5. Bibliography

[BAT 90] BATINA J., « Unsteady Euler Airfoil Solutions Using Unstructured Dynamic Meshes », *AIAA J.*, vol. 28, pp. 1381-1388, August 1990.

[BIS 57] BISPLINGHOFF R., ASHLEY H. and HALFMAN R., *Aeroelasticity*, Addison-Wesley, Reading, MA, USA, November 1957.

[FAR 95a] FARHAT C., « High Performance Simulation of Coupled Nonlinear Transient Aeroelastic Problems », AGARD Report R-807, Special Course on Parallel Computing in CFD (l'Aérodynamique numérique et le calcul en parallèle), North Atlantic Treaty Organization (NATO), October 1995.

[FAR 95b] FARHAT C., LESOINNE M. and MAMAN N., « Mixed Explicit/Implicit Time Integration of Coupled Aeroelastic Problems: Three-Field Formulation, Geometric Conservation and Distributed Solution », *Internat. J. Numer. Methods Fluids*, vol. 21, pp. 807-835, 1995.

[FAR 96] FARHAT C. and LESOINNE M., « On the Accuracy, Stability, and Performance of the Solution of Three-Dimensional Nonlinear Transient Aeroelastic Problems by Partitioned Procedures », AIAA paper 96-1388, In *37th AIAA/ASME/ASCE/AHS/ASC Structures, Structural Dynamics and Materials Conference, Salt lake City, Utah*, April 18-19 1996.

[FAR 98a] FARHAT C., DEGAND C., KOOBUS B. and LESOINNE M., « Torsional Springs for Two-Dimensional Dynamic Unstructured Fluid Meshes », *Comput. Methods Appl. Mech. Engrg.*, vol. 163, pp. 231-245, 1998.

[FAR 98b] FARHAT C., LESOINNE M. and LE TALLEC P., « Load and Motion Transfer Algorithms for Fluid/Structure Interaction Problems with Non-Matching Discrete Interfaces: Momentum and Energy Conservation, Optimal Discretization and Application to Aeroelasticity », *Comput. Methods Appl. Mech. Engrg.*, vol. 157, pp. 95-114, 1998.

[GUI 99] GUILLARD H. and FARHAT C., « On the Significance of the GCL for Flow Computations on Moving Meshes », AIAA paper 99-0793, In *AIAA 7th Aerospace Sciences Meeting and Exhibit, Reno, Nevada*, January 11-14 1999.

[GUP 96] GUPTA K., « Development of a Finite Element Aeroelastic Analysis Capability », *Journal of Aircraft*, vol. 33, pp. 995-1002, 1996.

[KOO 98] KOOBUS B. and FARHAT C., « Second-Order Implicit Schemes that Satisfy the GCL for Flow Computations on Dynamic Grids », AIAA paper 98-0113, In *36th Aerospace Sciences Meeting and Exhibit, Reno, Nevada*, January 12-15 1998.

[KOO 99] KOOBUS B. and FARHAT C., « Second-Order Time-Accurate and Geometrically Conservative Implicit Schemes for Flow Computations on Unstructured Dynamic Meshes », *Comput. Methods Appl. Mech. Engrg.*, vol. 170, pp. 103-129, 1999.

[LEE 93] LEE-RAUSCH E. M. and BATINA J. T., « Wing-flutter Boundary Prediction Using Unsteady Euler Aerodynamic Method », AIAA paper 93-1422, 1993.

[LES 93] LESOINNE M. and FARHAT C., « Stability Analysis of Dynamic Meshes for Transient Aeroelastic Computations », AIAA paper 93-3325, In *11th AIAA Computational Fluid Dynamics Conference, Orlando, Florida*, July 6-9 1993.

[LES 95] LESOINNE M. and FARHAT C., « Geometric Conservation Laws for Aeroelastic Computations Using Unstructured Dynamic Meshes », AIAA paper 95-1709, In *12th AIAA Computational Fluid Dynamics Conference, San Diego, California*, June 19-22 1995.

[LES 96] LESOINNE M. and FARHAT C., « Geometric Conservation Laws for Flow Problems with Moving Boundaries and Deformable Meshes, and Their Impact on Aeroelastic Computations », *Comput. Methods Appl. Mech. Engrg.*, vol. 134, pp. 71-90, 1996.

[LES 98] LESOINNE M. and FARHAT C., « A Higher-Order Subiteration Free Staggered Algorithm for Nonlinear Transient Aeroelastic Problems », *AIAA J.*, vol. 36, n° 9, pp. 1754-1756, 1998.

[MAM 86] MAMAN N. and FARHAT C., « Matching Fluid and Structure Meshes for Aeroelastic Computations: a Parallel Approach », *Comput. & Structures*, vol. 54, n° 4, pp. 779-785, 1986.

[MOU 96] MOURO J., « Numerical Simulation of Nonlinear Fluid Structure Interactions Problems and Application to Hydraulic Shock-Absorbers », In *Third World Conf. Appl. Computational Fluid Dynamics, Basel World User Days CFD*, May 19-23 1996.

[PIP 95] PIPERNO S., FARHAT C. and LARROUTUROU B., « Partitioned Procedures For The Transient Solution of Coupled Aeroelastic Problems », *Comput. Methods Appl. Mech. Engrg.*, vol. 124, n° 1-2, pp. 79-112, 1995.

[PIP 96] PIPERNO S., LARROUTUROU B. and LESOINNE M., « Analysis and Compensation of Numerical Damping in a One-Dimensional Aeroelastic Problem », *International Journal for Computational Fluid Dynamics*, vol. 6, pp. 157-174, 1996.

[PIP 97] PIPERNO S., « Explicit/Implicit Fluid/Structure Staggered Procedures with a Structural Predictor and Fluid Subcycling for 2D Inviscid Aeroelastic Simulations », *Internat. J. Numer. Methods Fluids*, vol. 25, pp. 1207-1226, 1997.

[PIP 99a] PIPERNO S. and FARHAT C., « An Energy Transfer Criterion for Assessing Partitioned Procedures Applied to the Solution of Non-linear Transient Aeroelastic Problems », In CAROSIO A., SMOLARKIEWICZ P., WILLAM K. and YANG J., Eds., *Fifth US National Congress on Computational Mechanics*, page 145, Boulder, Colorado, Aug. 4-6 1999. University of Colorado.

[PIP 99b] PIPERNO S. and FARHAT C., « Partitioned Procedures for the Transient Solution of Coupled Aeroelastic Problems. Part II: Energy Transfer Analysis and Three-Dimensional Applications », Rapport technique 99-03, Center for Aerospace Structures, University of Colorado, Boulder, Colorado, February 1999.

[PRA 94] PRAMONO E. and WEERATUNGA S., « Aeroelastic Computations for Wings Through Direct Coupling on Distributed-Memory MIMD Parallel Computers », AIAA paper 94-0095, In *32nd Aerospace Sciences Meeting and Exhibit*, Reno, Nevada, January 10-13 1994.

[STR 90] STRGANAC T. W. and MOOK D. T., « Numerical Model of Unsteady Subsonic Aeroelastic Behavior », *AIAA J.*, vol. 28, pp. 903-909, 1990.

[THO 79] THOMAS P. and LOMBARD C., « Geometric Conservation Law and Its Application to Flow Computations on Moving Grids », *AIAA J.*, vol. 17, pp. 1030-1037, October 1979.

[VAN 79] VAN LEER B., « Towards the Ultimate Conservative Difference Scheme V: a Second-Order Sequel to Godunov's Method », *J. Comput. Phys.*, vol. 32, pp. 361-370, 1979.

[YAT 87] YATES E. C.. « AGARD Standard Aeroelastic Configuration for Dynamic Response, Candidate Configuration I. - Wing 445.6 », NASA TM-100492, 1987.